Effect of S-doping on structural, optical and electrochemical properties of vanadium oxide thin films prepared by spray pyrolysis

M Mousavi[1], A Kompany[1,2], N Shahtahmasebi[1,2] and M-M Bagheri-Mohagheghi[3]

[1] Department of Physics, Ferdowsi University of Mashhad, Mashhad, Iran
[2] Nanoscience Center, Ferdowsi University of Mashhad, Mashhad, Iran
[3] School of Physics, Damghan University, Damghan, Iran

E-mail: m_mousavi1980@yahoo.com

Abstract

In this research, S-doped vanadium oxide thin films, with doping levels from 0 to 40 at.%, are prepared by spray pyrolysis technique on glass substrates. For electrochemical measurements, the films were deposited on florin–tin oxide coated glass substrates. The effect of S-doping on structural, electrical, optical and electrochemical properties of vanadium oxide thin films was studied. The x-ray diffractometer analysis indicated that most of the samples have cubic β-V_2O_5 phase structure with preferred orientation along [200]. With increase in the doping levels, the structure of the samples tends to be amorphous. The scanning electron microscopy images show that the structure of the samples is nanobelt-shaped and the width of the nanobelts decreases from nearly 100 to 40 nm with increase in the S concentration. With increase in the S-doping level, the sheet resistance and the optical band gap increase from 940 to 4015 kΩ/square and 2.41 to 2.7 eV, respectively. The cyclic voltammogram results obtained for different samples show that the undoped sample is expanded and the sample prepared at 20 at.% S-doping level has sharper anodic and cathodic peaks.

PACS numbers: 72.15.−v, 73.50.−h, 73.61.Le, 78.20.Jq, 78, 66, Li

(Some figures may appear in color only in the online journal)

1. Introduction

Vanadium oxide films, especially V_2O_5, have attracted considerable interest due to their unique features such as low cost and easy preparation, electrochemical activity, high stability and good specific energy [1, 2]. Vanadium oxide thin films have been used in fabricating many solid state devices, such as high-capacity lithium batteries, display systems, electrochromic (EC) devices (ECDs), electronic and optical switches and gas sensors. EC phenomenon, which can be observed for a range of transition metal oxides, is a reversible color change or, in general, a change in the optical properties during electrochemical oxidation or reduction processes [3].

Synthesis and fabrication of nanostructured vanadium oxides has recently been the subject of much research. It is known that V_2O_5, like many other materials, exhibits better electrochemical performance in the nanostructure form compared to bulk, since its morphology leads to slower electrochemical kinetics with high specific surface area and short diffusion distance. For example, V_2O_5 nanorod single-crystal arrays exhibit much improved electrochemical Li-ion intercalation properties in ECDs [2, 4]. It has been shown that different properties of V_2O_5 could be improved by introducing some guest cations into the material matrix. It has been reported that Ag^+, Cu^{2+}, Fe^{3+}, Al^{3+} and Na^+ enhance the electrochemical performance of this material [2, 5–8], and

besides, the band gaps of Ag, Nb and Na-doped vanadium oxides are superior to that of V_2O_5 [8]. All these ions replace vanadium cations, and to the best of our knowledge, not much work has been devoted to the replacement of oxygen ions.

In this work, we have studied the S-doped vanadium oxide films prepared by spray pyrolysis, for the first time. The influence of the deposition parameters on different properties of spray pyrolysis-prepared vanadium oxide films are being published elsewhere [9]. In this paper, the structural, electrical, optical and electrochemical properties of vanadium oxide nanoparticles with different S-doping levels have been studied. We expect sulfur to effectively modify the physical properties of vanadium oxide, since it can supersede the oxygen in this compound.

2. Experimental method

2.1. Film deposition

Undoped and S-doped vanadium oxide thin films were deposited on glass substrates and for the electrochemical measurements they were deposited on florin–tin oxide coated glass substrates by a spray pyrolysis technique. For the deposition of undoped film, a certain amount of vanadium chloride (VCl_3) was dissolved in distilled water to make the initial (precursor) solution. For doped films, the precursor solution was prepared by dissolving VCl_3 and different amounts of $(NH_2)_2CS$ in distilled water. The [S]/[V] atomic ratio was 0–40 at.%. The undoped and sulfur-doped V_2O_5 films (V_2O_5: S) were deposited under similar conditions. All the samples were deposited under a fixed nozzle to substrate distance (d) of 35 cm and compressed air pressure (P_{air}) of 3 atm as the carrier gas. All the samples were prepared at 0.1 M solution concentration (VCl_3) and solution spray of (R) = 5 ml min^{-1}. For undoped films, substrate temperature was kept constant at T_{sub} = 450 °C and for doped samples the substrate temperature was kept at 400 °C due to releasing the S^{2-} ions at high temperature to ambient.

2.2. Characterization

The structure of the prepared films were studied by x-ray diffraction technique (XRD) (D8 Advance Bruker system with Cu Kα, λ = 0.154 06 nm).

Surface morphology of the films was investigated by scanning electron microscopy (SEM) (VEGA TESCAN system). Optical measurements were carried out in the range of 300–1100 nm wavelength, using Unico 4802 spectrophotometer. The direct band gap (E_g) of the prepared films was obtained from the extrapolation of the linear part of $(\alpha h\nu)^2$ curve versus photon energy ($h\nu$), using the following equation [10]:

$$(\alpha h\nu)^2 = A(h\nu - E_g), \qquad (1)$$

where α is the absorption coefficient and A is a constant. The sheet resistance (R_s) of the films was measured by two-point probe method with Al electrodes made by thermal evaporation in vacuum, using Edwards E-306 coating system. The electrochromic measurments were performed in a cell containing the vanaduim oxide sample, a Pt counter-electrode
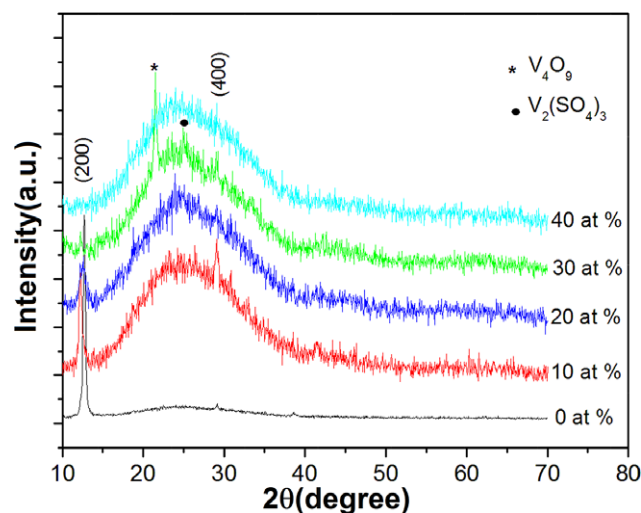
Figure 1. XRD patterns of vanadium oxide thin films with different S-doping levels from 0 to 40% in the solution.

and a Ag/AgCl reference electrode in a potential limit from -0.4 to $+1.2$ V at the scan rate of 50 mV s^{-1}. The electrolyte used was a solution of 1 M LiCl in distilled water.

## 3. Results and discussion

3.1. Structural properties

Figure 1 shows the XRD patterns of pure and S-doped vanadium oxide thin films with different doping levels from 10, 20, 30 and 40% in the solution. As seen, all the films are polycrystalline and the crystallographic peaks for films with 0, 10 and 20 at.% S-doping level belong to the cubic β-V_2O_5 phase with preferred orientation along [200] direction. The sample with 30 at.% S-doping level has V_4O_9 cubic phase with preferred orientation along [200]; the V_2 $(SO_4)_3$ phase has appeared in this sample. The sample with 40 at.% S-doping level has no obvious peak and is amorphous. The peak corresponding to [200] β-V_2O_5 is the strongest for the pure sample. The broadening of XRD peak corresponding to [200] β-V_2O_5 indicates that the crystallite size has decreased with increase in the doping level.

The SEM micrographs of the S-doped vanadium oxide thin films are shown in figures 2(a)–(e). The micrographs show that the nanostructure of the samples is nanorod- and nanobelt-shaped. The undoped vanadium oxide films show very clear nanorod and nanobelt shapes. It is worth mentioning that with increase in the S-doping levels from 0 to 40 at.%, the size of nanobelts and hence the corresponding grain size decreases and, to be more precise, their width reduces from nearly 100 to 40 nm.

3.2. Electrical property

The results of the electrical measurements of vanadium oxide thin films prepared at different S-doping levels with various thicknesses are given in table 1. The thickness of the films was determined from the transmission data (table 1) using Puma software [11]. The electrical measurements show that the sheet resistance of the films increases with increase in the S-doping levels from 0 to 40 at.%, which can be related to the
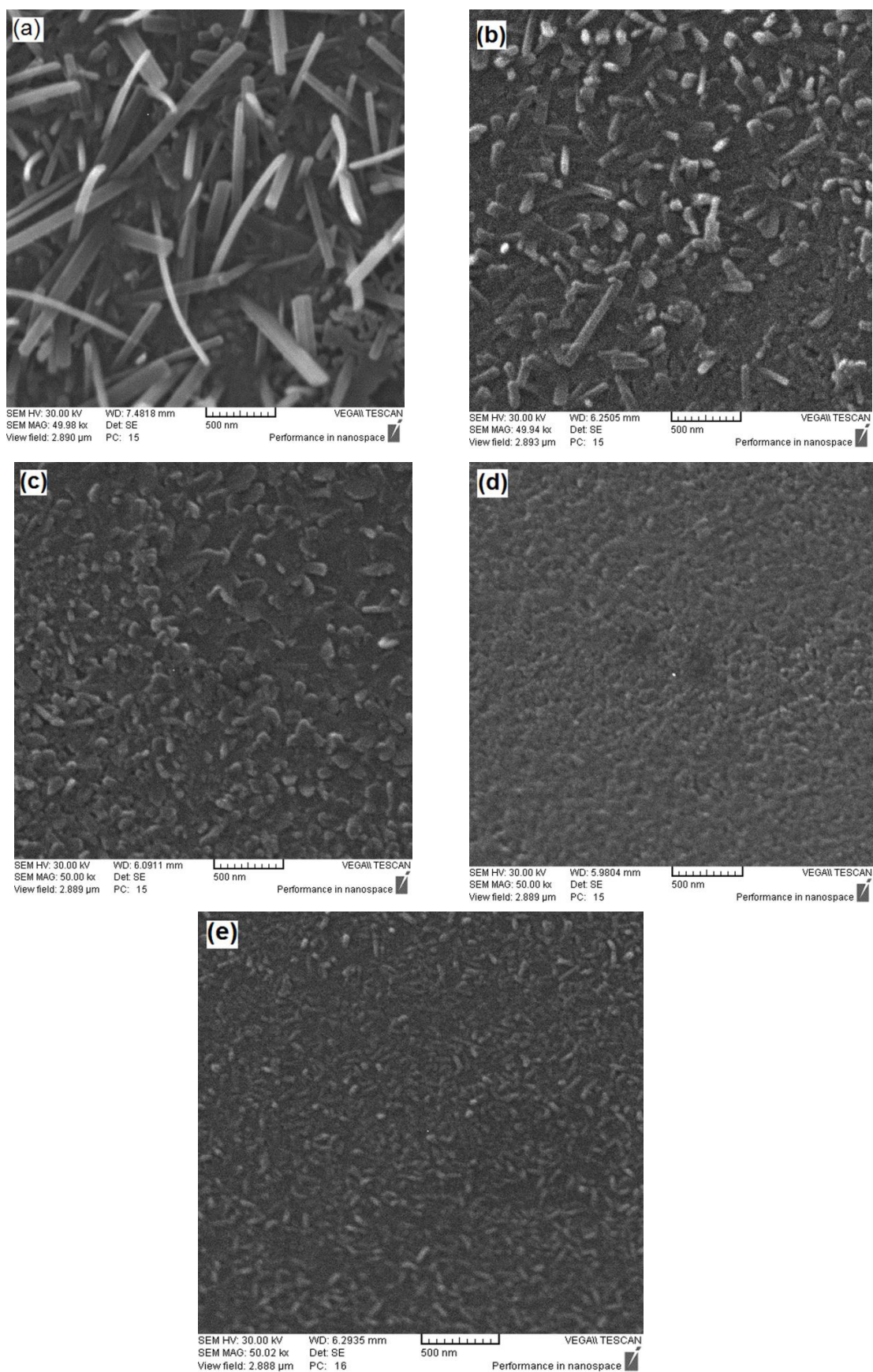
Figure 2. SEM images of vanadium oxide thin films (undoped as well as with various S-doping levels): (a) undoped vanadium oxide; (b) vanadium oxide with 10 at.% S-doping level; (c) vanadium oxide with 20 at.% S-doping level; (d) vanadium oxide with 30 at.% S-doping level; and (e) vanadium oxide with 40 at.% S-doping level.

**Table 1.** The electrical measurement results. (Thickness determination error is $\sim \pm 5\%$.)

Sample	R_s (kΩ/square)	Thickness (t) (nm)
Un-doped	940	110
10 at.%	1320	220
20 at.%	1650	260
30 at.%	2145	265
40 at.%	4015	270
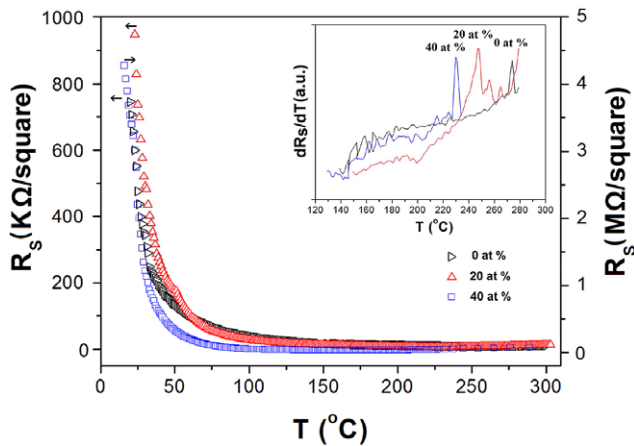
Figure 3. Plots of sheet resistance versus temperature for vanadium oxide with 0, 20 and 40 at.% S-doping levels, inset of figure 3 first derivative curves of sheet resistance versus temperature for vanadium oxide film with 0, 20 and 40 at.% S-doping levels.

decrease of the grain size and the amorphous structure. The temperature dependence of the resistance for the vanadium oxide thin films at 0, 20 and 40 at.% was measured. As seen in figure 3, first the resistance shows a decreasing trend and then begins to increase, without displaying the exact transition temperature. However, the transition points have been taken from the anomalies in their first derivative curves (the inset of figure 3). In this way, the phase transition from semiconductor to metallic one occurs at 274, 248 and 230 °C for the undoped films, films with S-doping level 20 at.% and films with S-doping level 40 at.%, respectively. With increase in the S-doping level, the temperature phase transition decreases.

3.3. Optical properties

Optical transmittances of the prepared films in the range of 300–1100 nm wavelength are shown in figure 4. The transmittance of the S-doped vanadium oxide films increases from ~33 to ~75% as the S-doping level increases from 10 to 40 at.%. This increasing trend may be due to the increasing band gap or equivalently, enhancing the insulating behavior of the films. It is confirmed considering the resistance behavior and also the microstructural features of the films. The considerable decrease in the absorbance edge of the sample with 30 at.% S content is due to the presence of a mixed oxide compound, as revealed by the XRD patterns which cause the sample to show more insulating behavior. The value of the band gap of the samples was obtained as depicted in figure 5, which shows that with the increase in the doping level of sulfur from 0 to 40 at.% the band gap increases from 2.41 to 2.7 eV, related to the grain size [12]. The considerable increase
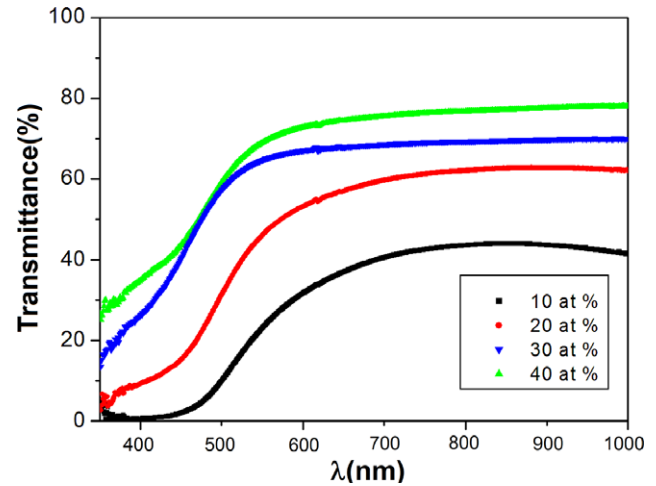
Figure 4. Optical transparency of S-doped vanadium oxide films deposited with different S concentrations.
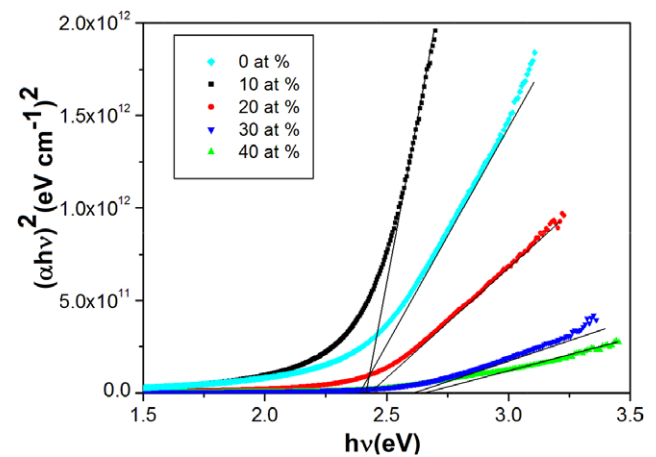
Figure 5. Plots of $(\alpha h\nu)^2$ versus $h\nu$ (photon energy) for undoped vanadium oxide sample and S-doped vanadium oxide films with different doping levels.

in the band gap of the sample with S-doping level 30 at.% is again related to the presence of a mixed oxide compound.

3.4. Electrochemical property

Figure 6 shows typical cyclic voltammograms (CV) of the fifth cycle of undoped and S-doped vanadium oxide thin films prepared with three layers in the potential region of -0.4 to $+1.2$ V versus Ag/Ag$^+$ with a scan rate of 50 mV s^{-1} in the solution of 1 M LiCl in distilled water. Figure 6(a) shows the CV of undoped vanadium oxide film. Two anodic peaks at $+0.02$ and $+0.31$ V and two cathodic peaks at -0.024 and -0.26 V are presented in the voltammogram. The color of the film is originally yellow and becomes green due to the presence of mixture ions V^{+4} and V^{+5} around 0 V, and then blue owing to the existence of V^{+4} ions at -0.4 V. As seen, the CV curve shows two-step electrochromism. Similar behavior has also been reported for V$_2$O$_5$ films [13]. Figure 6(b) shows the CV of S-doped at 20 at.% level in vanadium oxide film with two well-defined reduction peaks at ~ 0 and ~ -0.2 V and two oxidation peaks at ~ 0 and $\sim +0.2$ V. The CV of the S-doped sample at 40 at.% level in vanadium oxide is shown in figure 6(c). A similar shape of
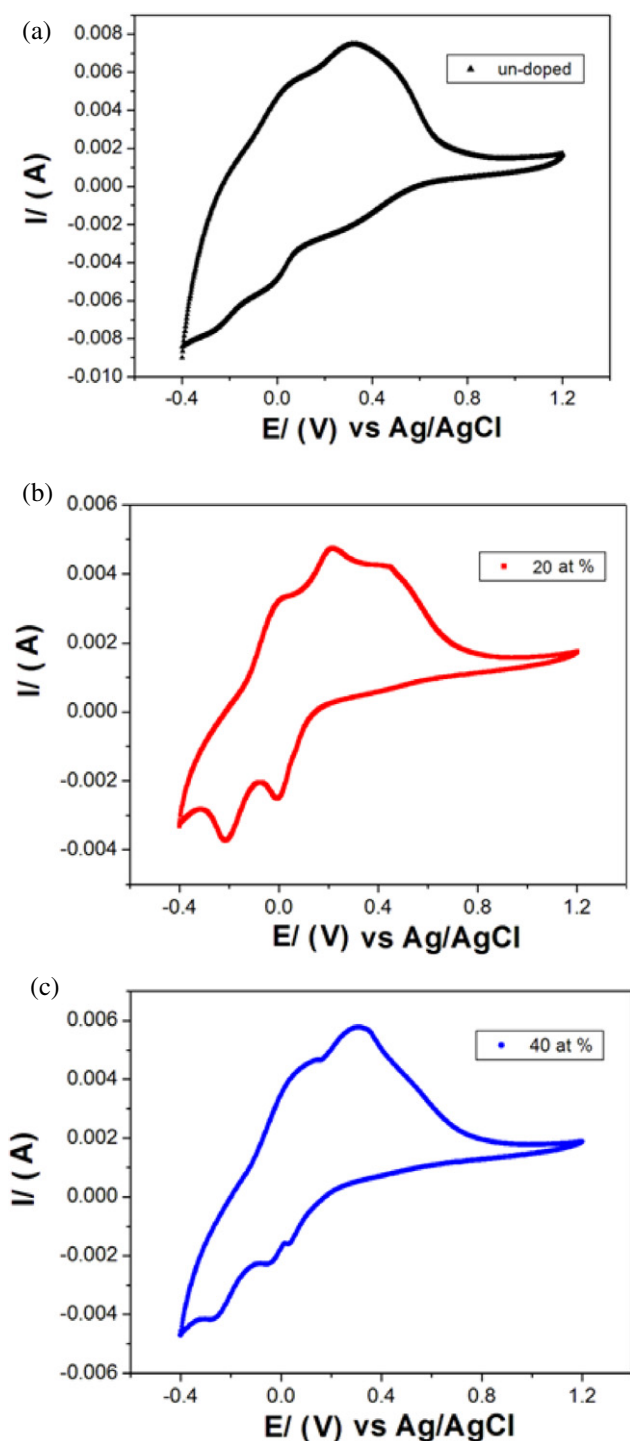
Figure 6. Cycle voltammetric of (a) vanadium oxide film and (b) vanadium oxide film with 20 at.% S-doping level and (c) vanadium oxide film with 40 at.% S-doping level, for fifth cycle. Potential scan rate 50 mV s^{-1}.

CV is observed compared to the S-doped film at 20 at.% level. The CV pattern shows two reduction peaks at ~ -0.04 and ~ -0.25 V and two oxidation peaks at $\sim +0.04$ and $\sim +0.3$ V. The color change behavior is similar to the undoped vanadium oxide samples, except that it is of a little darker color. The cathodic and anodic peaks in undoped vanadium oxide films are more expanded in comparison with the S-doping vanadium oxide sample. This is in contrast to the effect of Ta-doping which results in less resolved CV curve peaks [13]. As seen, the effect of S-doping in vanadium oxide thin films is a considerable decrease in the area of the CV. From this standpoint, the effect of S-doping in vanadium oxide is similar for Sm, Dy, Ag and Nd dopants. This behavior can be associated with the increase in the film resistance [8]. This is consistent with our electrical measurements, the results of which are reported in table 1. The difference in the potentials of anodic and cathodic peaks is almost similar for both the undoped and the doped samples; however, the peak in doped samples is more resolved compared to the undoped. This can be partially related to the change in the compound films and possibly to the morphology change [14]. As previously mentioned, with increasing S-doping level, the nanobelts and the corresponding grain size are decreased (figure 2). It is reasonable since the morphology of the nanostructured oxides or the total surface area of the nanostructured samples may affect the reaction rate in the EC experiment [15].

4. Conclusions

In this work, we investigate the effect of S-doping of different levels on the physical properties of vanadium oxide thin films prepared by spray pyrolysis. Our results revealed that S-doping in vanadium oxide thin films strongly affects its physical properties. By analyzing the obtained results, we have come to the following conclusions:

(a) Most of the prepared films show a preferential growth along the [200] direction with cubic β-V$_2$O$_5$ phase, except for the samples prepared with 30 and 40 at.% S-doping level. With increase in the level of doping, the [200] peak, corresponding to β-V$_2$O$_5$ phase, decreases to some extent, so that the structure of the sample with 40 at.% S-doped level is amorphous. The SEM micrographs show that by increasing the doping level from 0 to 40 at.%, the smaller nanobelts and nanorod shapes are formed.

(b) The temperature of the phase transition from semiconductor to metallic decreases with increase in the S-doping level.

(c) The transparency of the films increases from ~ 33 to $\sim 75\%$ as the S-doping level increases from 10 to 40 at.%. The optical band gap increases by increasing the S-doping level from 0 to 40 at.% as well, which is related to the grain size growth.

(d) From the CV curve results, it is clear that the area of the CV of the undoped vanadium oxide film is more expanded, which be related to the resistance of the films. The cathodic and anodic waves corresponding to the undoped vanadium oxide film are broader than that of the doped samples. So, the morphology of the prepared samples may affect the CV of the films.

References

[1] Patil C E, Tarwal N L, Shined P S, Deshmukh H P and Patil P S 2009 *J. Phys. D: Appl. Phys.* **42** 025404

[2] Zhan S, Wei Y, Bie X, Wang C, Du F, Chen G and Hu F 2010 *J. Alloys Compounds* **502** 92

[3] Nah Y C, Ghicov A, Kim D and Schmuki P 2008 *Electrochem. Commun.* **10** 1777

[4] Yu D M, Zhang S T, Liu D W, Zhou X Y, Xie S H, Zhang Q F, Liu Y Y and Cao G Z 2010 *J. Mater. Chem.* **20** 10841

[5] Coustier F, Passerini S and Smyrl W H 1997 *J. Solid State Ion.* **100** 247

[6] Giorgetti M, Berrettoni M and Smyrl W H 2007 *Chem. Mater* **19** 599

[7] Farcy J, Maingot S, Soudan P, Pereira-Ramos J P and Baffier N 1997 *Solid State Ion.* **99** 61

[8] Iida Y and Kanno Y 2009 *J. Mater. Process. Technol.* **209** 2421

[9] Mousavi M, Kompany A, Shahtahmasebi N and Bagheri-Mohagheghi M M 2013 *J. Mod. Phys. Lett.* B **27** 1350152

[10] Bagheri-Mohagheghi M M, Shahtahmasebi N, Alinejad M R, Youssefi A and Shokooh-Saremi M 2008 *Physica* B **403** 2431

[11] Birgin E G, Chambouleyron I and Martínez J M 1999 *J. Comput. Phys.* **151** 862

[12] Ramana C V, Smith R J, Hussain O M, Chusuei C C and Julien C M 2005 *Chem. Mater.* **17** 1213

[13] Avellaneda C O 2007 *Sci. Eng.* B **138** 118

[14] Kim Y T, Gopukumar S, Kim K B and Cho B W 2003 *J. Power Sources* **117** 110

[15] Cheng K C, Chen F R and Kai J J 2006 *Sol. Energy Mater. Sol. Cells* **90** 1156